

Relocation of Plastic Hinge of Interior Beam-Column Connections with Intermediate Bars in Reinforced Concrete and T-Section Steel Inserts in Precast Concrete Frames

P. Wongmatar, C. Hansapinyo, C. Buachart

Abstract—Failure of typical seismic frames has been found by plastic hinge occurring on beams section near column faces. On the other hand, the seismic capacity of the frames can be enhanced if the plastic hinges of the beams are shifted away from the column faces. This paper presents detailing of reinforcements in the interior beam-column connections aiming to relocate the plastic hinge of reinforced concrete and precast concrete frames. Four specimens were tested under quasi-static cyclic load including two monolithic specimens and two precast specimens. For one monolithic specimen, typical seismic reinforcement was provided and considered as a reference specimen named M1. The other reinforced concrete frame M2 contained additional intermediate steel in the connection area compared with the specimen M1. For the precast specimens, embedded T-section steels in joint were provided, with and without diagonal bars in the connection area for specimen P1 and P2, respectively. The test results indicated the ductile failure with beam flexural failure in monolithic specimen M1 and the intermediate steel increased strength and improved joint performance of specimen M2. For the precast specimens, cracks generated at the end of the steel inserts. However, slipping of reinforcing steel lapped in top of the beams was seen before yielding of the main bars leading to the brittle failure. The diagonal bars in precast specimens P2 improved the connection stiffness and the energy dissipation capacity.

Keywords—Relocation, Plastic hinge, Intermediate bar, T-section steel, Precast concrete frame.

I. INTRODUCTION

IN an earthquake event, concrete frame structures will be subjected to motions generating cyclic forces in the frame elements composing of beams and columns. The forces are systematically transferred along the elements through the rigid joint mechanism. In the most recent earthquakes, however, the often observed severe structural failure has been initiated by a damage or failure in the beam-column joint. The evident have obviously warned engineers of the importance of the joints [1] and a strict design procedure for keeping elastic behavior of the joint region has been codified in many seismic standards.

Due to the shortage of skilled labors in the construction industry and to achieve saving in cost and time, precast concrete construction has been widely adopted. The merit of using the precast construction is also the quality control under

factory based production protocol. Precast frame construction using beam and column elements is one of the precast systems. The module has advantages in flexible architectural adoptions, transportation compared to other types of precast systems i.e. precast wall. To emulate the traditional reinforced concrete frames which are monolithically made, quality of joint between the elements is needed to be carefully considered. Hence, many past researches have paid attentions on the joint behavior transferring loading path under seismic loading [2]-[7].

II. METHOD STATEMENT

A. Specimens and Material Properties

The experimental program comprised 4 interior beam-column specimens i.e., two monolithic specimen and two precast specimens. The monolithic specimen was seismically designed according to the ACI standard [8], [9] keeping strong column-weak beam failure mechanism (reference specimen M1) and input intermediate steel increased in joint and beam end area (specimen M2). For the two precast specimens, T-section steel inserts were embedded in the beam ends to transmit forces in beam-column connection area. The difference of the two specimens was without and with additional diagonal bars in connection area of P1 and P2, respectively. The details of RC and precast specimens were illustrated in Fig. 1. The identical detail of beam was used in both RC and precast. For the column detail between RC and precast were made different because the aim of usability.

Fig. 2 showed the erection processes of the precast specimens. The column bellowing the connection was prepared with four corner reinforced steel having thread ends. For the two side beams, the T-section steel inserts were embedded in the beam ends at the bottom level. In the erection process, the steel inserts were extended in the connection area and the two opposite steel inserts were connected together with a welded lapping plate. The internal force in the top steel of the beams was transferred using lapped steels with provided overlapping length. The precast column above the connection was connected by a steel socket as shown in Fig. 3. Table I shows tensile strength of reinforcing bars and the steel insert. The specimen types and concrete cylindrical compressive strengths are illustrated in Table II.

F. P. Wongmatar, S. C. Hansapinyo, and T. C. Buachart are with the Department of Civil Engineering, Chiang Mai University, Thailand (e-mail: piyapong_wongmatar@hotmail.com, chayanon@eng.cmu.ac.th, chinapat@eng.cmu.ac.th).

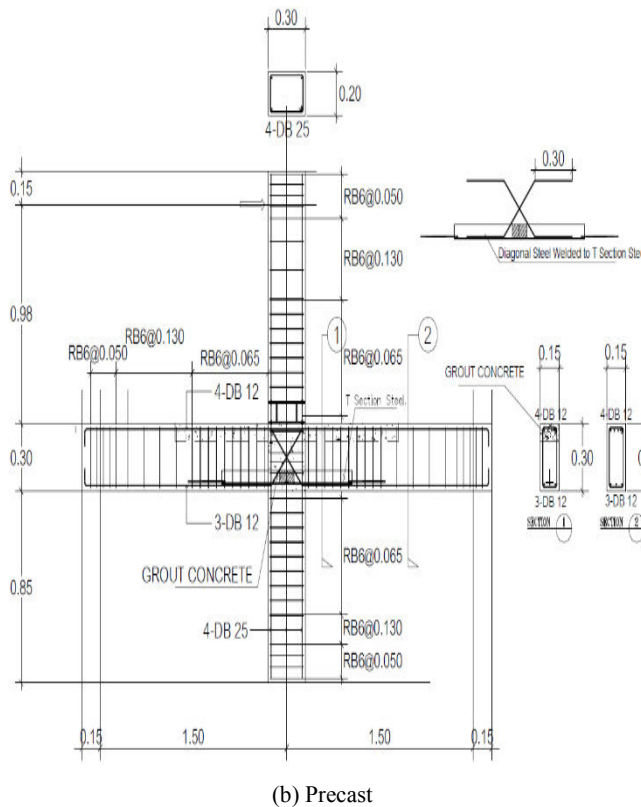
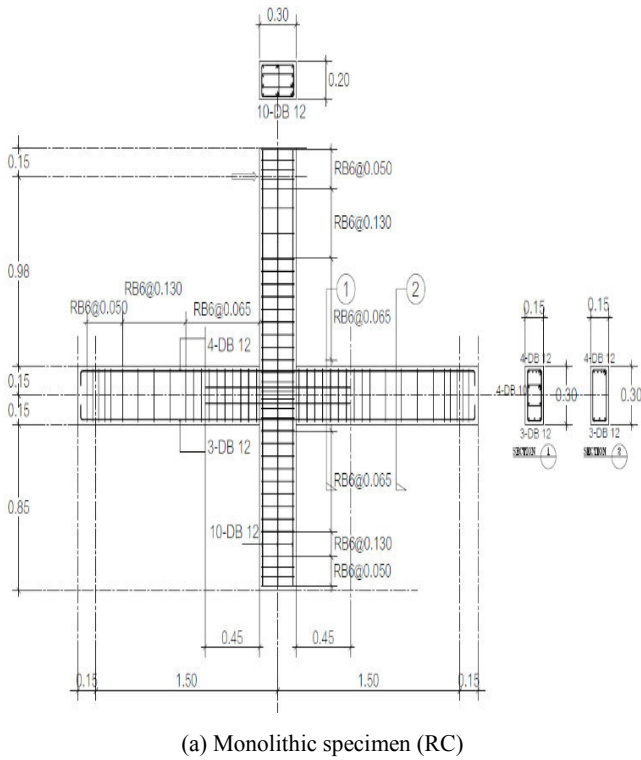


Fig. 1 Details of the test specimens (Unit: m)

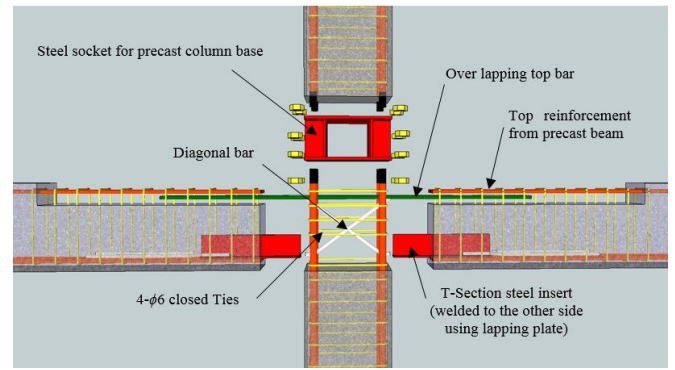


Fig. 2 Precast specimen (P1, P2)

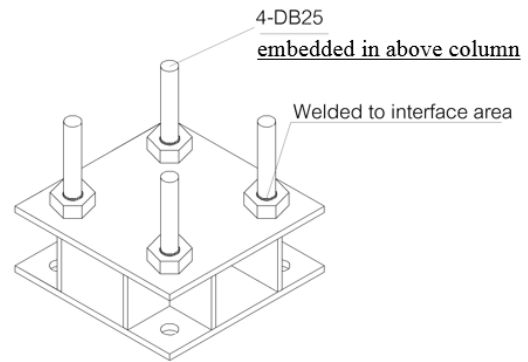


Fig. 3 Steel plate for connected column elements

TABLE I
 PROPERTIES OF REINFORCED STEEL

| Type | Yield strength (MPa) | Ultimate strength (MPa) |
|-------------|----------------------|-------------------------|
| RB6 | 365 | 542 |
| DB10 | 546 | 769 |
| DB12 | 418 | 572 |
| DB25 | 443 | 686 |
| Steel plate | 282 | 384 |

TABLE II
 COMPRESSIVE STRENGTH OF CONCRETES

| Sample | Specimen Type | Element | Compressive strength(MPa) |
|--------|---------------|---------|---------------------------|
| M1,M2 | Monolithic | All | 44 |
| P1 | Precast | Beam | 43 |
| | | Column | 45 |
| | | Joint | 57 |
| P2 | Precast | Beam | 43 |
| | | Column | 45 |
| | | Joint | 46 |

B. Test Set-Up

Sub-assembly frame emulating interior joint behavior of a sway frame building under seismic loading was set up as shown in Fig. 4. The columns above and below the connection were at mid-story each representing half-length columns. The side beams were also the half-bay beams. The bottom end of the column was supported by a hinge and the ends of the beams were supported by rollers. The boundary configuration allows the tested frame to be able to sway under the lateral loading, similar to moment frame buildings under earthquake attack. The axial compressive load with magnitude of 10% of

column axial capacity was applied to column by a hydraulic jack and kept constant throughout the testing. The lateral cyclic load was applied at the top of the column using displacement control scheme. The targets of lateral drift ratio, defined as Δ/h , for all specimens were conducted conforming to the ACI T1.1 [10] recommendation, as shown in Fig. 5. Three cycles of loading were repeated for each lateral drift target.

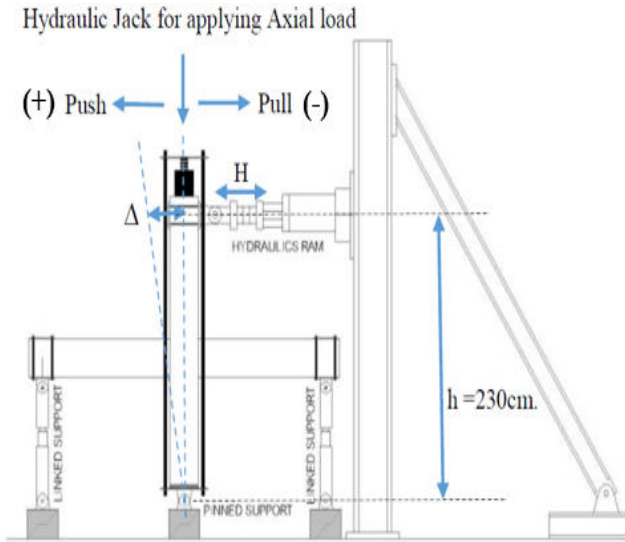


Fig. 4 Test set-up

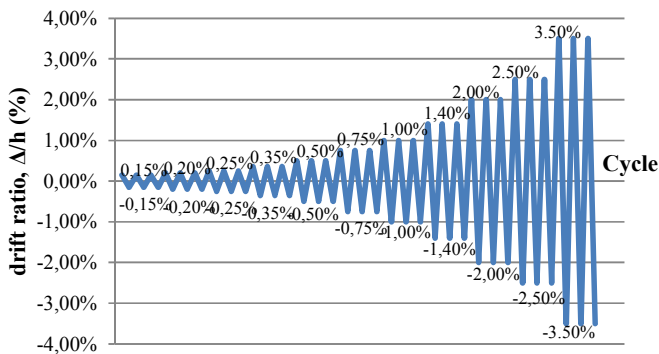
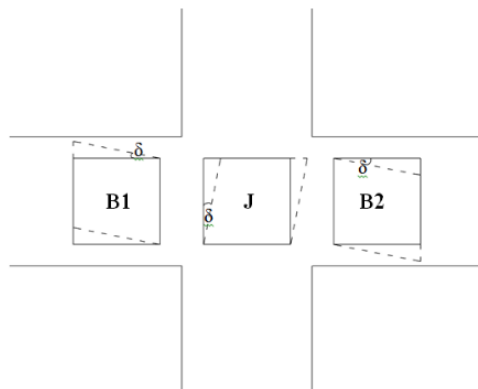
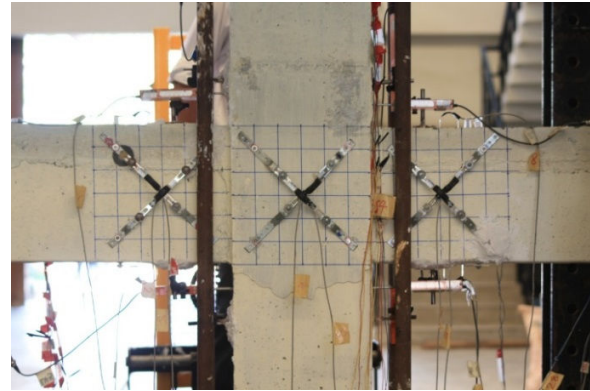


Fig. 5 Displacement history



(a) Shear deformation



(b) Tool measurement

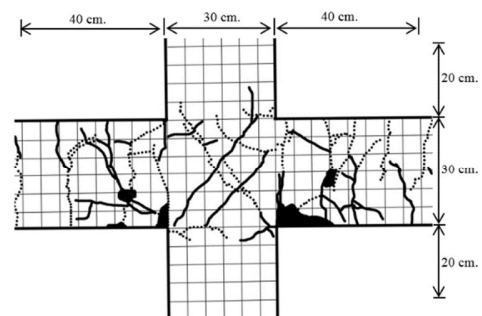
Fig. 6 Test measurements

The test specimens were white painted skin with 5x5 cm grids for crack development observation during the tests. The measurements during the test, as shown in Fig. 6, include measurement 1) shear deformation in beams and connection areas 2) rocking angle at the column face and 3) strains of longitudinal steels in beams.

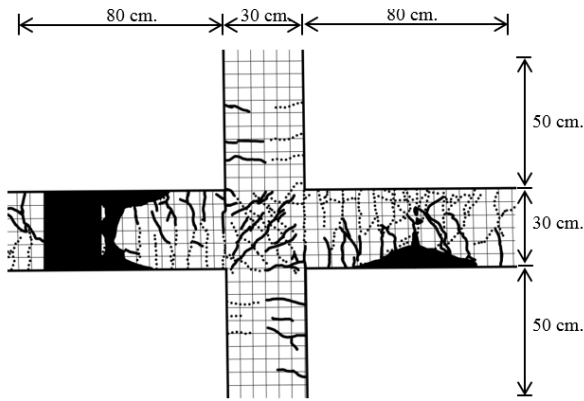
III. EXPERIMENTAL RESULTS AND DISCUSSION

A. Damage Observation

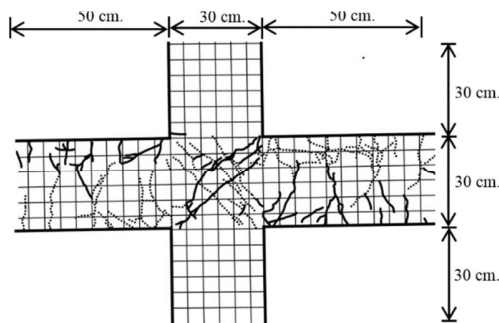
The sequence of damage in all specimens was indicated in this part. First with M1, the flexural crack in beam was observed in early test. Then the flexural crack and diagonal crack continued to grow in sizes (length and opening). The feature of plastic hinge was seen in beam end beside column face with crushing and spalling of concrete cover. The occurring damage of M2, contained additional intermediate steel in the connection area, was different to M1. The severe damage occurred in beam always form joint which was the end point of intermediate steel so this character brought plastic hinge in beam. For precast specimens, the slipping of reinforcing steel lapped in top of the beams was the cause of failure in both specimens (P1 and P2) which the cracks parallel the lapped bar were obviously seen. Nevertheless, P2 experienced diagonal crack in joint less than P1 since the diagonal bar that was added only in its. The crack feature in beam in precast specimens had trend to always form connection but it not showed clearly because the slipping failure.



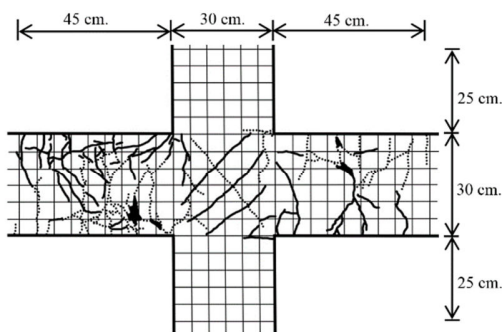
(a) Specimen M1



(b) Specimen M2



(c) Specimen P1



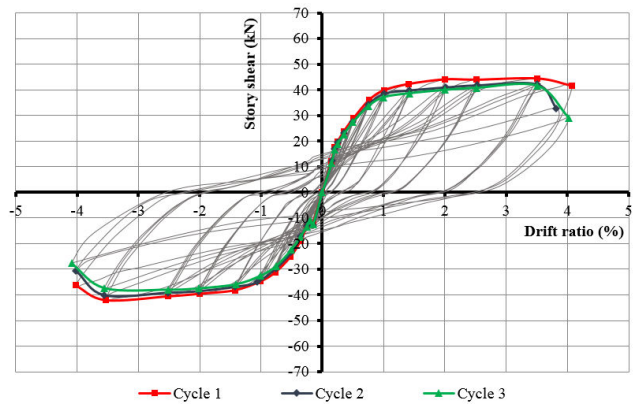
(d) Specimen P2

Fig. 7 Specimens after failure (Rigid and broken line respectively indicate cracks under right and left swaying directions)

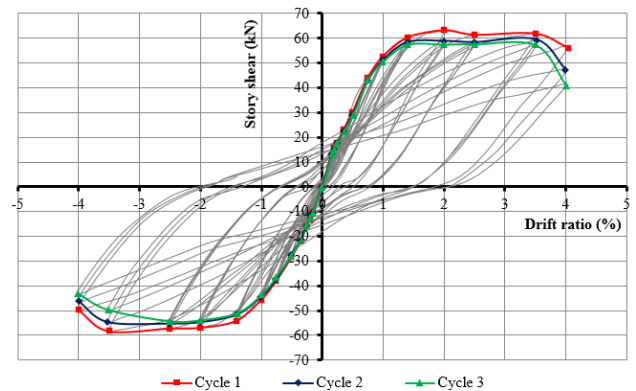
B. Hysteretic Loops

The column shear force–drift ratio relationships and hysteretic loops are shown in Fig. 8 that repeated 3 cycles in each displacement. The positive and negative direction was shown in Fig. 4 (positive and negative is push and pull respectively). For M1, the distinctive decrease in stiffness was found after the yielding of flexural reinforcement at about 1.0% drift ratio. Then, the specimen could not resist more shear force. However, the post-peak behavior was stable maintaining the shear force during the 1.4 – 3.5% drift ratios. The strength peaked and dropped after 3.5% drift ratio, the maximum shear force was 43 kN. With the yielding failure, the M1 specimen showed wide hysteretic loop which influenced to large energy dissipation. In Fig. 8 (b), the M2 had the trend of graph like M1 and it had the most stiffness

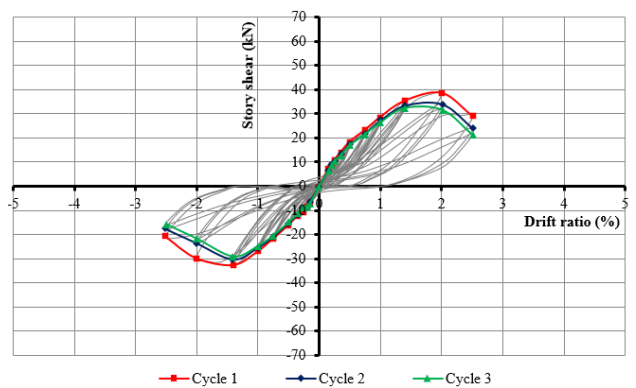
and strength which the maximum shear force was 63 kN. The differential between RC and precast specimen was the aspect of hysteretic loop and post-peak behavior. The narrow loop was shown in precast specimens. For two precast specimens showed in Figs. 8 (c) and (d) are P1 and P2 respectively. Both specimens indicate immediate decrease of shear force after peak load. This form often can be induced to brittle failure which not appropriate in seismic structure. The envelope curve of precast specimens illustrated the peak load at 38 and 42 kN for P1 and P2, respectively.



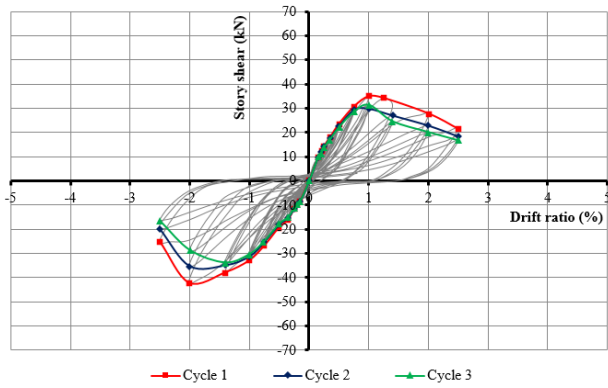
(a) Specimen M1



(b) Specimen M2



(c) Specimen P1

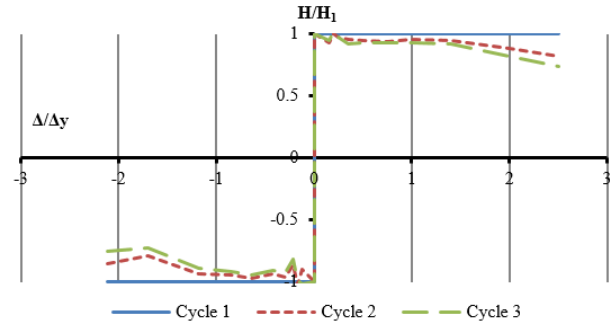


(d) Specimen P2

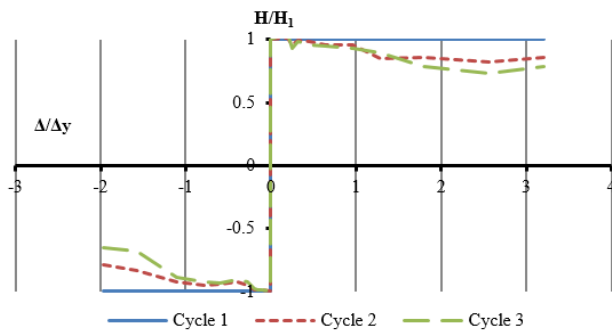
Fig. 8 Column shear force – drift ratio relation

C. Abbreviations and Acronyms

With the repetition of the cyclic loading in each drift ratio, the strength degradation could be found, especially in the range of large drift. The strength degradation of the test specimens were shown in Fig. 9. The Y-axis represented the ratio of between the story shear at each repetitive cycle and at the first cycle. The X-axis represents the ratio between lateral drift and yielding drift. The yielding drift is defined as Park recommended [12], were 1.0%, 1.1%, 1.2% and 1.0% drift ratio for specimens M1, M2, P1 and P2 respectively. The degradation of all specimens started when ratio of drift more than 1. The monolithic specimen had little strength degradation until the drift of about 3-4 times of the yielding drift (Figs. 8 (a), (b)). For the precast specimens, the degradation could be obviously seen after the yielding drift (Figs. 8 (b), (c)).



(c) Specimen P1



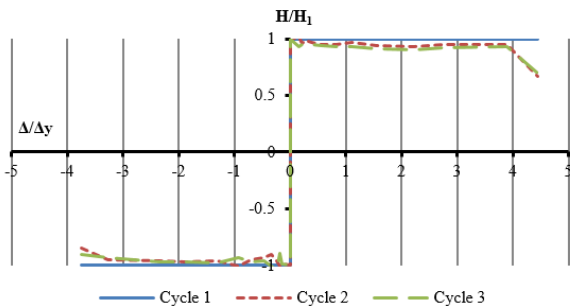
(d) Specimen P2

Fig. 9 Strength Degradation

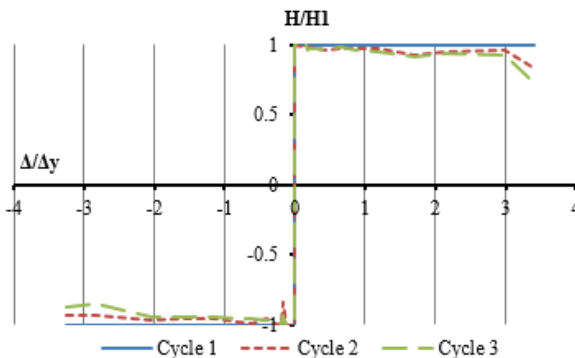
D. Shear Deformation and Rocking Angle

The shear deformations measured in term of shear distortional angle, as shown in Fig. 6. For Fig. 10, the x and y axes are % drift ratio and the rotation angle in radian, respectively. The deformations in the beam end area and in the joint area were compared in the figure. For a clear presentation, the envelop deformation curve of the first cycle was used to show and B2 region (Fig. 6 (a)) was chosen for representative of the beam end area. For the M1 specimen, at the early state, the shear deformations in beam end area and joint area increased linearly with the higher rate in the joint area. However, after 2.00% drift ratio, the large axial deformation after the yielding of the flexural reinforcement with intensive damage occurring in beam end area induced the rapid increase in the shear deformation of the area [11], [12]. Nevertheless, the shear deformation in the joint area was stable increasing linearly with the drift ratio (Fig. 10 (a)). The improvement of shear distortion due to the presence of the intermediate steel in M2 was demonstrated in Fig. 10 (b). For the precast specimens, the shear deformation was very little. This is due to the premature failure of the rebar slipping. However, the addition of diagonal bars in the joint area of specimen P2 tended to decrease the shear deformation in the joint.

Fig. 11 shows measurement of rocking angle related to the column movement. The story shear – rocking angle relation at column face was compared in Fig. 12. In early loading, the damage occurred at beam end and the rocking angle was small until the damage occurred in joint. The specimen M2 containing damage in beam away from joint, hence the

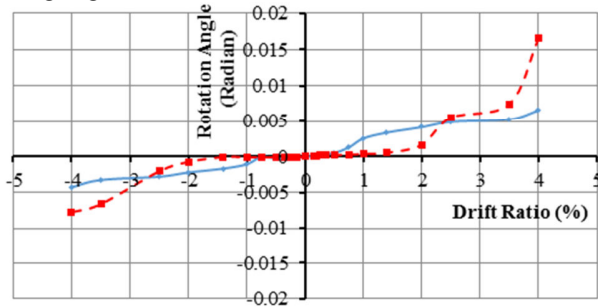


(a) Specimen M1



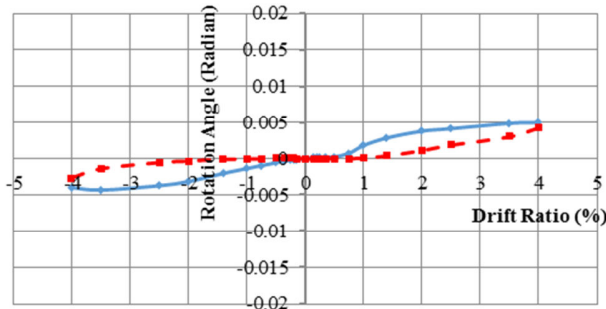
(b) Specimen M2

rocking angle was less.



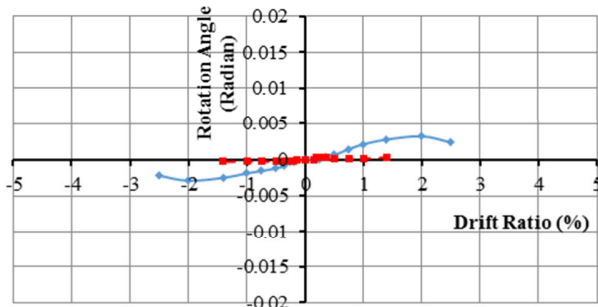
— Zone J - - - Zone B2

(a) Specimen M1



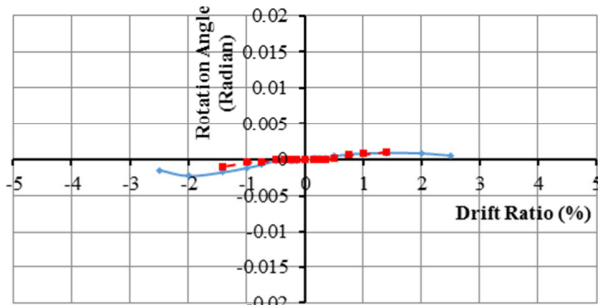
— Zone J - - - Zone B2

(b) Specimen M2



— Zone J - - - Zone B2

(c) Specimen P1



— Zone J - - - Zone B2

(d) Specimen P2

Fig. 10 Shear deformation and joint and beam end areas

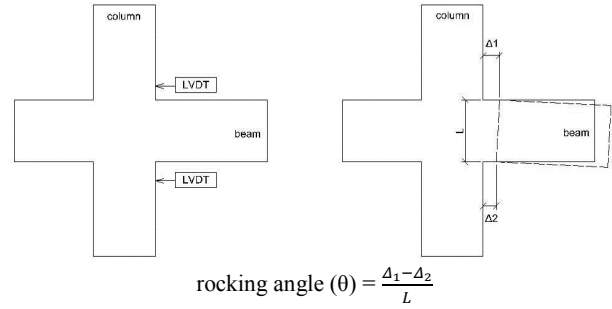


Fig. 11 Position to measure rocking angle

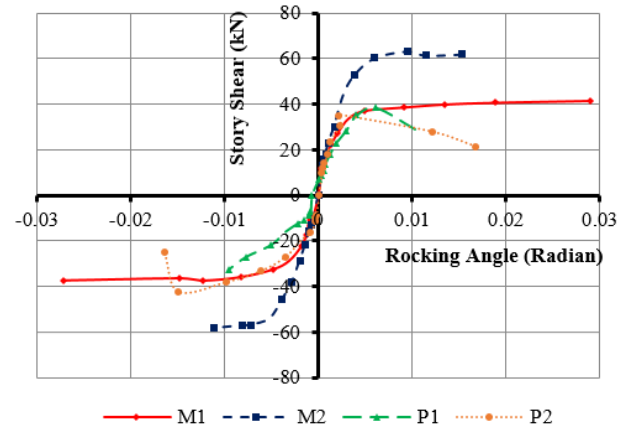


Fig. 12 Rocking Angle

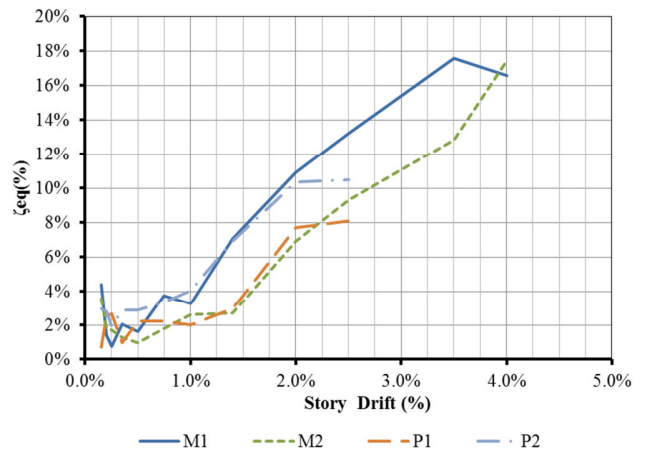


Fig. 13 Energy dissipation

E. Energy Dissipation

Fig. 13 shows equivalent viscous damping ratio (ζ_{eq}) [13]. The specimen P1 possessed the least energy dissipation with narrow hysteretic loop (Fig. 7 (c)). The specimen P2 had quantity of energy dissipation more than P1 because of the presence of diagonal bars in joint region. The monolithic specimen M1 had larger energy dissipation compared to that of specimen M2. This is due to the yielding of specimen M1 was generated before M2, but at ultimate state the quantity of dissipation for the specimens was equal.

F. Ductility

Ductility based on the Park guideline [14] was adopted to

determine the quantity of ductility as shown in Fig. 14. The results are showed in Table III. The positive means push and negative means pull (Fig. 4). The specimen M1 had the highest ductility and P1 had lowest value. Due to the premature failure of slipping of rebar, the precast specimens were with lower ductility.

TABLE III
 DUCTILITY

| Specimen | Ductility (d_u/d_y) | | |
|----------|-------------------------|----------|---------|
| | Positive | Negative | Average |
| M1 | 4.44 | 4.08 | 4.26 |
| M2 | 3.46 | - | 3.46 |
| P1 | 1.77 | 1.92 | 1.84 |
| P2 | 2.51 | 1.80 | 2.15 |

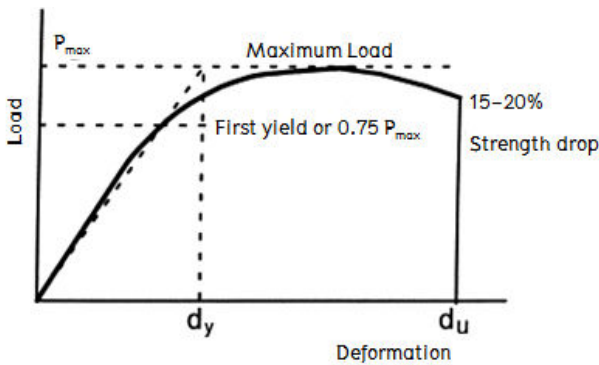


Fig. 14 Method to evaluate ductility [14]

G. Strains in Reinforced Steel

The strain information of each drift ratios which received from strain meters attached on reinforcing bars are presented here. The positions of strain meters in each specimens were demonstrated in Figs. 15, 17, 19 and 21 for specimens M1, M2, P1 and P2, respectively. For specimen M1, the largest strain shown in Fig. 16 occurred only at point 8. The large strain was consistent with damage generating plastic hinge that occurred on the beam end beside the column face. The plastic hinge of M2 occurred far from the beam end and hence the strain values are not as many as those of specimen M1, as seen in Fig. 18. For precast specimens P1 and P2, as seen in Figs. 20 and 22, the strains were lower than yielding strain of the reinforcing steel. However, the strain values were higher at the location shifted away from the beam ends. Hence, the improvement of lapping details will make the precast developing higher shear strength. Especially, in P2 specimen that illustrated the little quantity of strain in the reinforcing steel.

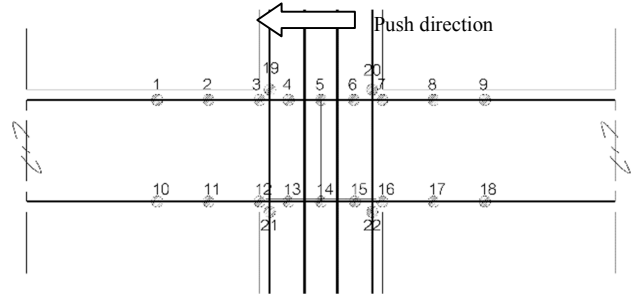


Fig. 15 Strain meter position in M1

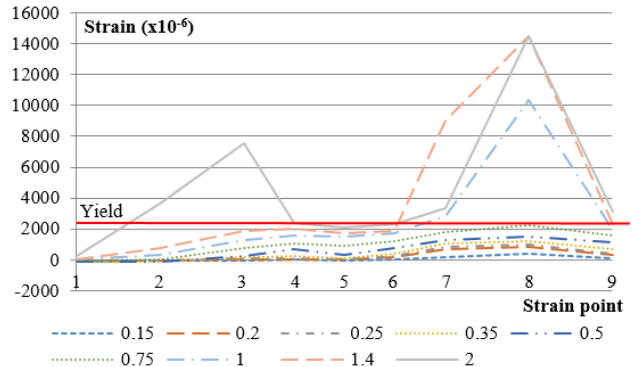


Fig. 16 Strain result in top beam steel on M1

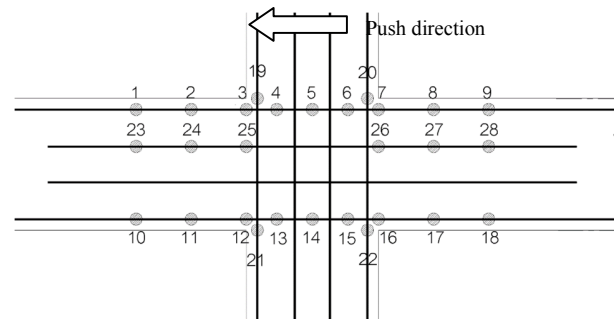


Fig. 17 Strain meter position in M2

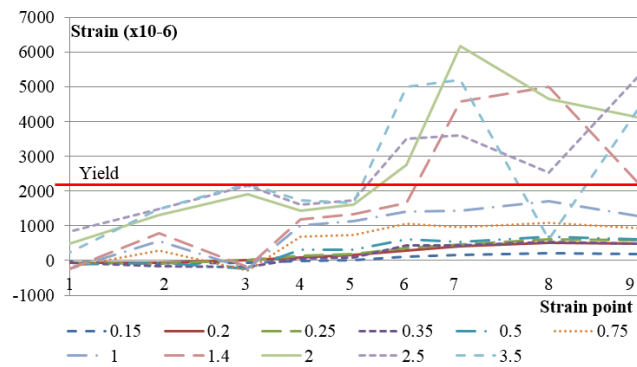


Fig. 18 Strain result in top beam steel on M2

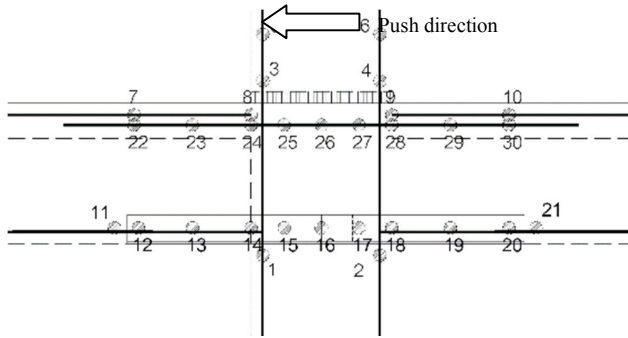


Fig. 19 Strain meter position in P1

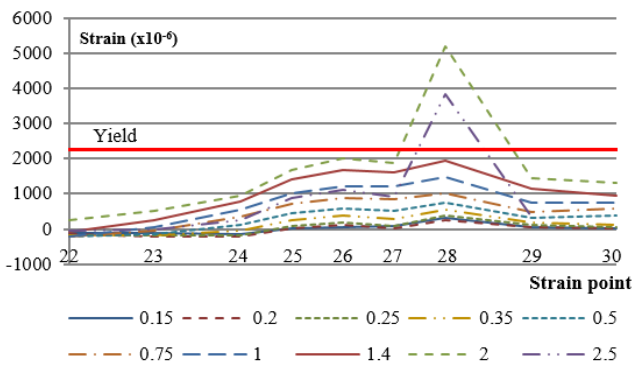


Fig. 20 Strain result in top beam steel on P1

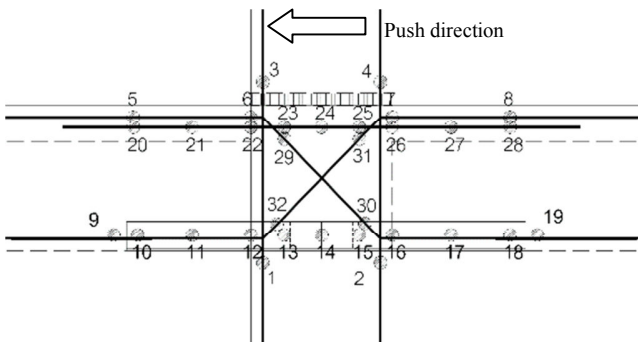


Fig. 21 Strain meter position in P2

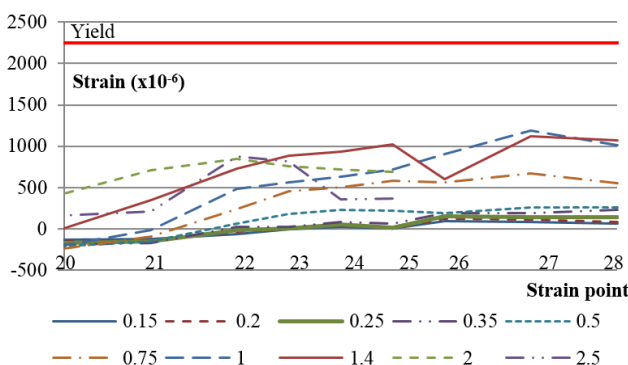


Fig. 22 Strain result in top beam steel on P2

IV. CONCLUSION

This paper presents detailing of reinforcements in the interior beam-column connections aiming to relocate the

plastic hinge of two reinforced concrete and two precast concrete frames. The four specimens were tested under quasi-static cyclic load. Additional intermediate rebar and T-section steel inserts were provided for shifting the plastic hinge of the reinforced concrete and precast concrete specimens, respectively. The test results indicated the ductile failure with beam flexural failure in monolithic specimen M1 and the intermediate steel increased strength and improved joint performance of specimen M2. For the precast specimens, cracks generated always form joint region. However, slipping of reinforcing steel lapped in top of the beams was seen before yielding of the main bars leading to the brittle failure. The diagonal bars in precast specimens P2 improved the connection stiffness and the energy dissipation capacity. The precast can develop shear strength if the lapped detail is improved.

ACKNOWLEDGMENT

The authors would like to acknowledge Chiang Mai University for financial support under Ph.D. scholarship.

REFERENCES

- [1] Xilin L, et al, "Seismic behavior of interior RC beam-column joint with additional bars under cyclic loading," *Earthquakes and Structures*, Vol.3, No.1, 2012, pp.37-57.
- [2] Sergio, M., Rene C., David, P. and Raul, M., "Seismic Tests of Beam-to-Column Connections in a Precast Concrete Frame," *PCI Journal*, May-June 2002, pp.70-89.
- [3] Park, R., "The FIB State-of-the-Art Report on the Seismic Design of Precast Concrete Building Structure," 2003 Pacific Conference on Earthquake Engineering, Paper Number 011.
- [4] Svetlana, B. and Teresa, G., "Precast Concrete Construction, World Housing Encyclopedia," 2011
- [5] Daniel, C., "Finite Element Analysis of Precast Prestressed Beam-Column Concrete Connection in Seismic Construction," Master's Thesis, Department of Civil and Environmental Engineering, Chalmers University of Technology., 2006.
- [6] Lu, X., Urukup, T.H., Li, S. and Lin, F., "Seismic Behavior of Interior RC Beam-Column Joints with Additional Bars under Cyclic Loading," *Earthquakes and Structures*, 2012, Vol.3, No.1, pp.37-57.
- [7] Au, F.T.K., Huang, K. and Pam, H.J., "Diagonally-Reinforced Beam-Column Joints Reinforced Under Cyclic Loading," *Structures & Buildings*, 158, Issue SB1, 2005, pp. 21-40.
- [8] ACI Committee 318, 318-05/318R-05, "Building Code Requirements for Structural Concrete and Commentary," American Concrete Institute, Farmington Hills, MI., 2005.
- [9] ACI Committee 352, 352R-02, "Recommendation for Design of Beam-Column Joints in Monolithic Reinforced Concrete Structures," American Concrete Institute, Farmington Hills, MI., 2002.
- [10] ACI Committee 374, "Acceptance Criteria for Moment Frames Based on Structural Testing," T1.1-01/T1.1R-01, Farmington Hills, MI., 2001.
- [11] Hansapinyo, C. Pimanmas, A., Maekawa, K. and Chaisomphob, T. (2003) "Proposed Model of Shear Deformation of Reinforced Concrete Beam after Diagonal Cracking," *J. of Materials, Conc. Struct., Pavements*, Vol.58 (Feb), No.725, pp.321-332.
- [12] Lee, J., Kim, J., and Oh, G., "Strength Deterioration of Reinforced Concrete Beam-Column Joints Subjected to Cyclic Loading," *Engineering Structure*, Vol.31, 2009, pp.2070-2085.
- [13] Chopra, A. K., "Theory and Applications to Earthquake Engineering: Dynamic of Structure (Third Edition)," Prentice Hall, Englewood Cliffs, NJ. 2000.
- [14] Park, R., Evaluation of Ductility of Structures and Structural Assemblages from Laboratory Testing, *Bulletin of the New Zealand National Society for Earthquake Engineering*, 1989, Vol.22, No.3, pp. 155-166.

Mr. Piyapong Wongmatar is currently Ph.D. student at Department of Civil Engineering, Chiang Mai University. He received M.Eng. in Civil Engineering in 2012 from Department of Civil Engineering, Chiang Mai University, Thailand. His specialties are related to structural mechanics and earthquake resistant design.

Dr. Chayanon Hansapinyo received Ph.D. in Civil Engineering in 2005 from Sirindhorn International Institute of Technology, Thammasat University, Thailand. He is now working as Assistant Professor at Department of Civil Engineering, Chiang Mai University. His specialties are related to structural mechanics and earthquake resistant design.

Dr. Chinapat Buachart received Ph.D. in Civil Engineering in 2013 from Asian Institute of Technology (AIT), Thailand. He is now working as lecturer at Department of Civil Engineering, Chiang Mai University. His specialties are related to structural mechanics and finite element analysis.